Table S1. Longitude range for each latitude range used in the interpolation over NA and EU. For longitudinal ranges in EU spanning across 0°/360°, it is implied this longitude is included (e.g., 350-1 = 10°W- 1°E).

North America (NA)[a]		*Europe (EU)*[b]	
Latitude range (°N, southern-northern edge)	Longitude range (°E, western-eastern edge)	Latitude range (°N, southern-northern edge)	Longitude range (°E, western-eastern edge)
25-26	278-280	36-37	352-358
26-27	260-263; 277-280	37-38	351-360; 12-17; 21-24
27-28	260-263; 277-280	38-39	350-1; 8-24
28-29	259-265; 277-280	39-40	350-1; 8-24
29-30	255-280	40-41	351-2; 8-24; 26-29
30-31	254-280	41-42	351-3; 8-30
31-32	247-280	42-43	350-3; 8-29
32-33	242-281	43-44	350-29
33-34	241-282	44-45	355-30
34-35	239-284	45-46	355-31
35-36	238-285	46-47	355-31
36-37	238-285	47-48	355-31
37-38	237-285	48-49	355-30
38-39	236-285	49-50	354-29
39-40	236-286	50-51	354-28
40-41	235-288	51-52	349-28
41-42	235-290	52-53	349-28
42-43	235-290	53-54	349-29
43-44	235-292	54-55	349-29
44-45	235-293	55-56	351-30
45-46	235-293	56-57	352-31
46-47	235-293	57-58	352-31
47-48	235-293	58-59	353-32
48-49	235-293	59-60	356-33
		60-61	357-33
		61-62	4-33
		62-63	5-33
		63-64	7-34
		64-65	11-32
		65-66	12-32
		66-67	13-32
		67-68	17-32
		68-69	18-32
		69-70	20-31
		70-71	23-28

[a]Western (WNA) and eastern (ENA) North America is split by 264°E
[b]Southern (SEU) and northern (NEU) Europe is split by 53°N

Table S2. Summary statistics for the observations (OBS), ACCMIP models (A-H), and UCI CTM (I) with respect to summer (JJA) and winter (DJF) diurnal cycles.

Data	Metric, description (unit)	OBS	A	B	C	D	E	F	G	H	I
WNA diurnal summer (JJA)	*h,* maximum phase (hour)	15.3	16.6	16.6	16.5	15.4	15.3	14.9	15.2	16.0	12.9
	H, peak-to-peak amplitude (ppb)	26.8	28.4	17.7	20.3	22.8	20.6	18.1	11.5	17.9	34.4
	MB, mean bias (ppb)	-	3.6	10.8	-0.5	5.1	2.4	4.6	5.9	14.7	20.0
	R, cycle correlation	1.00	0.92	0.92	0.94	0.99	1.00	0.98	0.99	0.97	0.75
	NSD, normalized standard deviation	1.00	1.07	0.69	0.75	0.84	0.76	0.67	0.43	0.69	1.33
ENA diurnal summer (JJA)	*h,* maximum phase (hour)	15.0	17.0	16.1	16.5	15.5	15.8	15.2	15.7	16.0	12.7
	H, peak-to-peak amplitude (ppb)	29.1	28.3	28.4	21.8	22.7	21.8	22.6	12.1	18.5	54.0
	MB, mean bias (ppb)	-	19.0	24.4	1.1	12.2	3.5	17.9	21.1	12.9	37.0
	R, cycle correlation	1.00	0.87	0.95	0.92	0.99	0.97	0.98	0.96	0.95	0.75
	NSD, normalized standard deviation	1.00	0.99	0.99	0.74	0.78	0.75	0.77	0.44	0.66	1.95
SEU diurnal summer (JJA)	*h,* maximum phase (hour)	15.5	16.4	16.6	16.4	15.1	15.6	15.3	15.5	16.3	13.1
	H, peak-to-peak amplitude (ppb)	24.3	31.9	20.3	18.8	21.3	16.2	15.0	12.9	15.3	36.0
	MB, mean bias (ppb)	-	17.0	17.8	5.2	16.8	1.0	12.4	21.8	14.3	31.5
	R, cycle correlation	1.00	0.96	0.94	0.97	0.99	1.00	0.99	0.99	0.97	0.74
	NSD, normalized standard deviation	1.00	1.33	0.87	0.77	0.87	0.67	0.62	0.54	0.65	1.54
NEU diurnal summer (JJA)	*h,* maximum phase (hour)	15.1	17.1	16.7	16.5	15.0	16.0	15.6	16.2	15.8	14.4
	H, peak-to-peak amplitude (ppb)	13.9	15.8	11.2	10.0	11.1	8.2	9.0	7.2	8.7	13.1
	MB, mean bias (ppb)	-	15.9	11.2	4.9	13.8	0.9	8.8	12.7	3.7	23.5
	R, cycle correlation	1.00	0.86	0.90	0.93	1.00	0.96	0.99	0.94	0.97	0.97
	NSD, normalized standard deviation	1.00	1.16	0.82	0.72	0.80	0.59	0.65	0.53	0.64	0.95
WNA diurnal winter (DJF)	*h,* maximum phase (hour)	14.8	17.1	17.9	16.0	14.8	15.0	15.6	14.0	16.8	16.7
	H, peak-to-peak amplitude (ppb)	9.8	11.5	5.9	8.8	7.5	6.2	7.9	3.7	6.0	13.2
	MB, mean bias (ppb)	-	6.4	16.7	14.4	6.8	2.0	6.1	23.6	13.6	8.2
	R, cycle correlation	1.00	0.76	0.69	0.92	0.98	0.97	0.95	0.95	0.88	0.83
	NSD, normalized standard deviation	1.00	1.06	0.54	0.80	0.69	0.58	0.73	0.35	0.60	1.18
ENA diurnal winter (DJF)	*h,* maximum phase (hour)	15.1	18.0	16.7	15.7	15.3	14.0	15.9	14.8	16.3	16.1
	H, peak-to-peak amplitude (ppb)	9.1	6.7	7.5	11.3	7.8	5.8	6.9	2.4	10.6	12.6
	MB, mean bias (ppb)	-	10.2	13.2	9.8	-1.5	-4.6	4.0	30.1	5.5	4.8
	R, cycle correlation	1.00	0.72	0.90	0.98	0.99	0.92	0.97	0.97	0.95	0.92
	NSD, normalized standard deviation	1.00	0.72	0.76	1.16	0.82	0.61	0.71	0.25	1.12	1.26
SEU diurnal winter (DJF)	*h,* maximum phase (hour)	15.1	17.6	17.8	16.1	15.0	14.2	15.8	14.7	16.4	16.4
	H, peak-to-peak amplitude (ppb)	5.1	3.5	3.5	6.7	4.2	2.5	3.9	1.4	5.1	10.8
	MB, mean bias (ppb)	-	8.3	17.5	18.4	8.6	5.7	9.6	27.7	12.5	12.7
	R, cycle correlation	1.00	0.71	0.71	0.90	0.93	0.86	0.91	0.95	0.91	0.82
	NSD, normalized standard deviation	1.00	0.95	0.53	1.04	0.67	0.41	0.60	0.23	0.83	1.63
NEU diurnal winter (DJF)	*h,* maximum phase (hour)	4.5	17.8	6.5	14.9	14.5	13.3	15.3	12.2	15.0	16.2
	H, peak-to-peak amplitude (ppb)	0.2	1.5	0.2	1.5	1.1	0.9	0.8	0.4	1.5	2.4
	MB, mean bias (ppb)	-	-2.7	13.8	15.4	2.3	-1.4	0.0	26.9	6.2	8.2
	R, cycle correlation	1.00	0.27	-0.72	0.50	0.54	0.27	0.40	0.24	0.45	0.32
	NSD, normalized standard deviation	1.00	1.01	0.27	1.06	0.83	0.63	0.52	0.28	1.05	1.56

Table S3. Summary statistics for the observations (OBS), ACCMIP models (A-H), and UCI CTM (I) with respect to the annual cycle of MDA8.

Data	Metric, description (unit)	OBS	A	B	C	D	E	F	G	H	I
WNA annual MDA8	m, maximum phase (month)	5.6	5.5	4.9	3.3	5.4	5.6	5.6	1.5	6.6	6.0
	M, peak-to-peak amplitude (ppb)	21.7	16.7	13.0	12.4	20.4	20.6	15.9	5.0	18.3	37.0
	MB, mean bias (ppb)	-	6.9	10.6	6.9	4.7	-0.5	2.4	10.0	10.6	15.5
	R, cycle correlation	1.00	0.96	0.90	0.36	0.98	1.00	0.99	-0.49	0.86	0.97
	NSD, normalized standard deviation	1.00	0.82	0.66	0.68	0.94	0.94	0.74	0.24	0.88	1.71
	$\bar{E}_{JJA}$, 87th – 30th percentile (ppb)	19.7	19.5	14.5	16.4	17.9	17.2	15.1	17.5	18.5	29.7
	$R_{E\text{-}JJA}$, spatial correlation of E_{JJA} maps	1.00	0.54	0.59	0.28	0.43	0.47	0.59	0.17	0.61	0.63
ENA annual MDA8	m, maximum phase (month)	5.3	5.8	6.0	3.7	5.8	5.7	6.1	6.0	6.2	6.3
	M, peak-to-peak amplitude (ppb)	20.7	29.8	29.1	12.8	32.7	25.9	31.5	3.5	20.3	64.6
	MB, mean bias (ppb)	-	16.9	16.6	6.8	4.2	-4.2	8.1	20.1	8.0	24.8
	R, cycle correlation	1.00	0.95	0.90	0.57	0.96	0.96	0.93	0.56	0.89	0.86
	NSD, normalized standard deviation	1.00	1.47	1.45	0.83	1.57	1.24	1.51	0.28	1.03	3.08
	$\bar{E}_{JJA}$, 87th – 30th percentile (ppb)	22.8	33.0	27.5	19.4	27.0	22.4	28.3	19.1	21.9	56.1
	$R_{E\text{-}JJA}$, spatial correlation of E_{JJA} maps	1.00	0.70	0.81	0.52	0.69	0.69	0.34	0.27	0.69	0.71
SEU annual MDA8	m, maximum phase (month)	5.5	5.8	5.6	4.0	5.8	5.5	5.7	6.7	6.2	5.9
	M, peak-to-peak amplitude (ppb)	26.3	37.9	22.7	14.6	33.8	17.4	24.9	11.9	21.0	49.4
	MB, mean bias (ppb)	-	15.6	16.2	13.0	11.4	1.3	8.1	21.1	11.2	23.7
	R, cycle correlation	1.00	0.98	1.00	0.66	0.98	0.99	0.97	0.78	0.91	0.97
	NSD, normalized standard deviation	1.00	1.45	0.86	0.64	1.27	0.66	0.94	0.49	0.84	1.87
	$\bar{E}_{JJA}$, 87th – 30th percentile (ppb)	23.6	30.1	18.0	16.7	24.9	15.2	20.9	14.8	18.8	37.9
	$R_{E\text{-}JJA}$, spatial correlation of E_{JJA} maps	1.00	0.33	0.71	0.15	0.77	0.54	0.46	0.24	0.65	0.62
NEU annual MDA8	m, maximum phase (month)	4.3	5.6	3.9	2.7	5.5	4.7	5.4	1.1	3.9	5.6
	M, peak-to-peak amplitude (ppb)	17.4	32.8	14.0	18.3	22.7	12.4	19.3	10.4	8.3	26.2
	MB, mean bias (ppb)	-	8.3	12.2	11.8	7.0	-2.0	2.1	19.1	4.6	15.1
	R, cycle correlation	1.00	0.78	0.97	0.64	0.82	0.96	0.82	0.00	0.88	0.78
	NSD, normalized standard deviation	1.00	1.87	0.82	1.21	1.29	0.71	1.09	0.67	0.57	1.48
	$\bar{E}_{JJA}$, 87th – 30th percentile (ppb)	15.8	30.5	15.3	19.5	17.7	13.4	17.6	14.4	13.3	20.9
	$R_{E\text{-}JJA}$, spatial correlation of E_{JJA} maps	1.00	0.51	0.50	-0.39	0.63	0.63	0.66	0.11	0.23	0.63

Table S4. Summary statistics for the observations (OBS), ACCMIP models (A-H), and UCI CTM (I) with respect to the annual cycle of AQX events and AQX episodes (NA and EU combined, 100 AQX events per decade case).

Data	Metric, description (unit)	OBS	A	B	C	D	E	F	G	H	I
WNA AQX events	m_{AQX}, maximum phase (month)	6.1	5.9	4.6	3.0	4.9	6.0	6.1	1.7	7.5	6.5
	R, AQX cycle correlation	1.00	0.85	0.41	-0.24	0.57	0.97	0.96	-0.07	0.64	0.78
	NSD, normalized standard deviation	1.00	0.53	0.65	1.74	1.15	1.01	1.06	0.57	1.35	1.58
	R_{MDA8}, correlation of AQX and MDA8 cycles	0.81	0.82	0.89	0.91	0.80	0.82	0.77	0.59	0.78	0.69
	$\bar{E}_{AQX}$, AQX threshold – 30th percentile (ppb)	27.6	29.2	20.6	26.9	24.4	23.7	21.5	25.4	26.7	43.2
	$R_{E\text{-}AQX}$, spatial correlation of E_{AQX} maps	1.00	0.66	0.66	0.40	0.49	0.35	0.56	0.36	0.55	0.62
ENA AQX events	m_{AQX}, maximum phase (month)	5.5	6.2	6.8	3.2	6.2	6.4	6.6	6.8	7.7	6.6
	R, AQX cycle correlation	1.00	0.80	0.65	0.04	0.88	0.79	0.76	0.70	0.36	0.65
	NSD, normalized standard deviation	1.00	1.11	1.44	1.90	1.22	1.27	1.29	1.03	1.25	1.48
	R_{MDA8}, correlation of AQX and MDA8 cycles	0.84	0.76	0.78	0.88	0.78	0.82	0.80	0.78	0.70	0.83
	$\bar{E}_{AQX}$, AQX threshold – 30th percentile (ppb)	34.7	53.8	39.9	29.1	36.1	30.4	41.1	32.1	31.5	82.3
	$R_{E\text{-}AQX}$, spatial correlation of E_{AQX} maps	1.00	0.70	0.78	0.28	0.63	0.53	0.44	0.60	0.74	0.68
SEU AQX events	m_{AQX}, maximum phase (month)	6.0	6.2	6.0	3.2	5.8	5.8	6.0	6.8	7.3	6.3
	R, AQX cycle correlation	1.00	0.97	0.96	-0.09	0.88	0.96	0.93	0.78	0.64	0.90
	NSD, normalized standard deviation	1.00	0.99	1.11	1.68	1.30	0.96	1.19	1.17	1.40	1.33
	R_{MDA8}, correlation of AQX and MDA8 cycles	0.81	0.79	0.76	0.84	0.73	0.84	0.82	0.90	0.74	0.80
	$\bar{E}_{AQX}$, AQX threshold – 30th percentile (ppb)	33.9	46.3	24.3	25.1	30.8	21.5	30.2	26.3	29.3	57.4
	$R_{E\text{-}AQX}$, spatial correlation of E_{AQX} maps	1.00	0.33	0.70	0.12	0.66	0.42	0.20	0.07	0.58	0.51
NEU AQX events	m_{AQX}, maximum phase (month)	4.3	5.5	3.9	3.2	5.3	4.6	5.6	4.2	4.4	5.9
	R, cycle correlation	1.00	0.46	0.84	0.67	0.46	0.86	0.46	0.19	0.98	0.29
	NSD, normalized standard deviation	1.00	0.81	0.85	1.57	1.18	0.88	0.99	0.91	0.74	1.14
	R_{MDA8}, correlation of AQX and MDA8 cycles	0.87	0.84	0.93	0.85	0.73	0.93	0.85	0.26	0.90	0.74
	$\bar{E}_{AQX}$, AQX threshold – 30th percentile (ppb)	23.9	45.8	20.6	29.1	23.3	19.5	29.1	21.8	17.9	31.6
	$R_{E\text{-}AQX}$, spatial correlation of E_{AQX} maps	1.00	0.51	0.55	-0.47	0.54	0.53	0.55	0.53	0.45	0.60
NA AQX episodes	$\bar{S}$, weighted geometric mean AQX episode size (10^4 km^2-days)	415	128	229	1426	461	290	522	243	774	463
	CCD_{100}, fraction of AQX events' areas in AQX episodes > 100 x 10^4 km^2-days (%)	79.0	56.1	73.7	92.6	85.3	76.1	80.3	73.0	83.0	80.2
	CCD_{1000}, fraction of AQX events' area in AQX episodes > 1000 x 10^4 km^2-days (%)	38.0	9.7	12.8	69.2	30.8	19.2	43.6	12.7	48.7	37.5
	$\Delta\bar{E}_S$, average increase in E_S for AQX episodes of size S (ppb-dec^{-1})	2.9	9.9	4.6	0.8	2.3	2.9	-0.1	3.5	2.9	6.0
EU AQX episodes	$\bar{S}$, weighted geometric mean AQX episode size (10^4 km^2-days)	444	173	198	2106	656	290	616	498	606	535
	CCD_{100}, fraction of AQX events' areas in AQX episodes > 100 x 10^4 km^2-days (%)	80.1	63.1	70.6	92.8	82.0	74.1	85.1	82.3	83.5	84.4
	CCD_{1000}, fraction of AQX events' area in AQX episodes > 1000 x 10^4 km^2-days (%)	34.9	18.1	15.2	70.0	53.7	23.7	51.5	46.5	49.6	39.8
	$\Delta\bar{E}_S$, average increase in E_S for AQX episodes of size S (ppb dec^{-1})	1.7	8.3	2.9	1.5	2.4	2.0	3.9	2.3	4.6	6.9

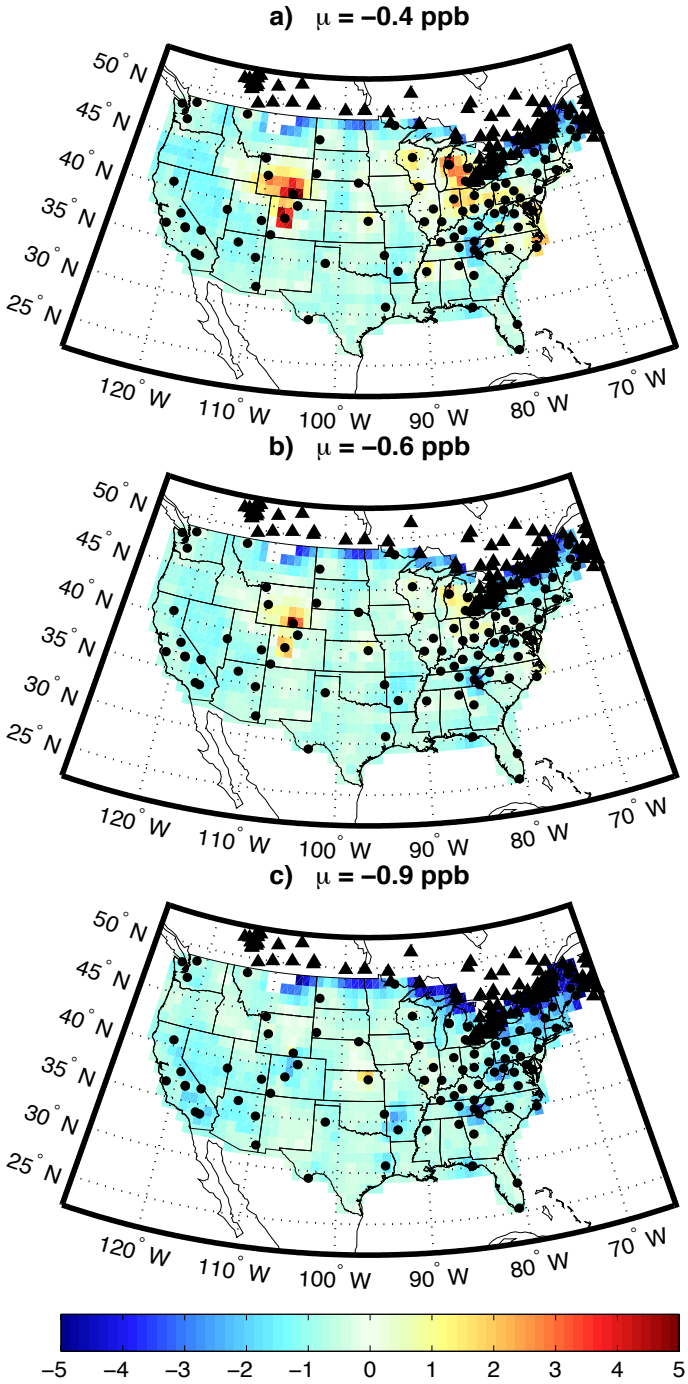

Figure S1. Change in the MDA8 O_3 (ppb) corresponding to the (**a**) 25th, (**b**) 50th, and (**c**) 95th percentiles over NA, shown as the datasets used in this analysis (AQS + CASTNet + NAPS) minus the dataset used in Schnell et al., (2014) (AQS only). The locations of the CASTNet (circles) and NAPS (triangles) stations and the domain area-weighted average difference are shown for each panel.

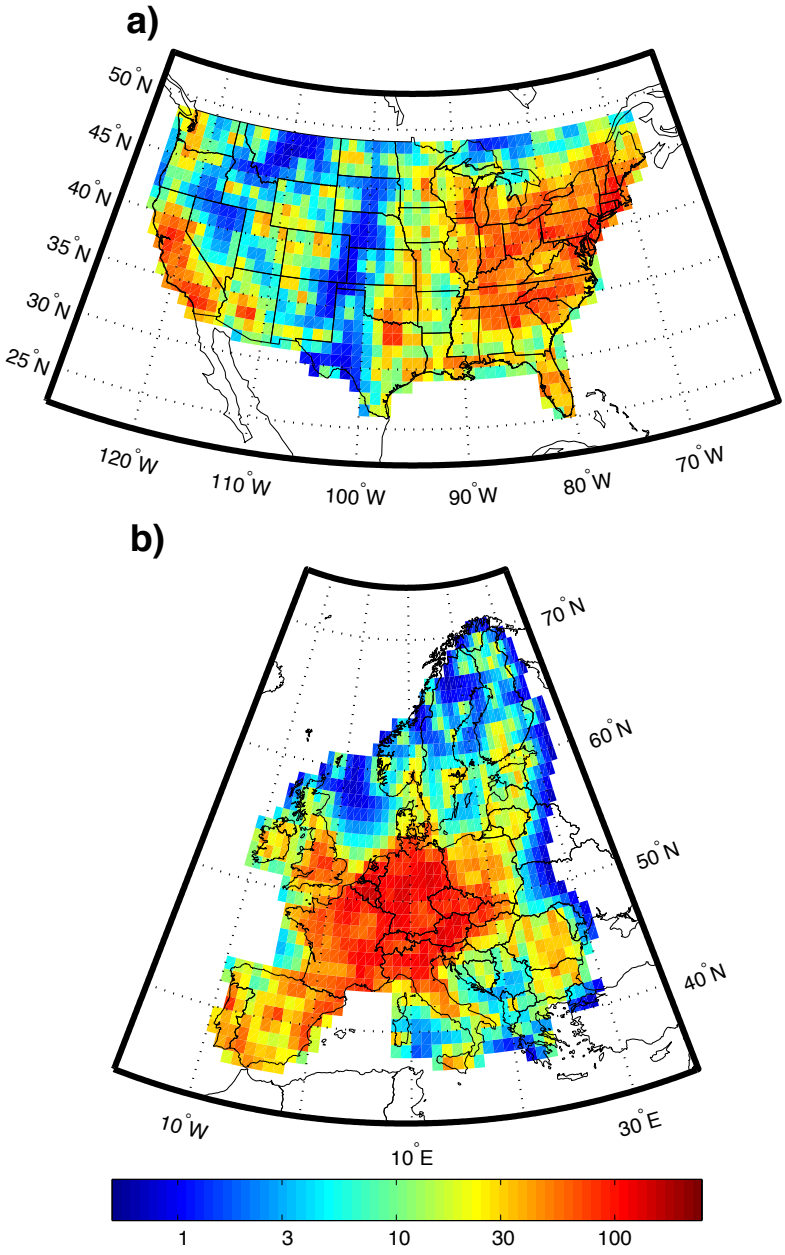

Figure S2. Quality of prediction index (Q^P, see S2014) for the interpolation of the 2000-2009 observations over (**a**) NA and (**b**) EU. Note the log-scale of the colorbar.

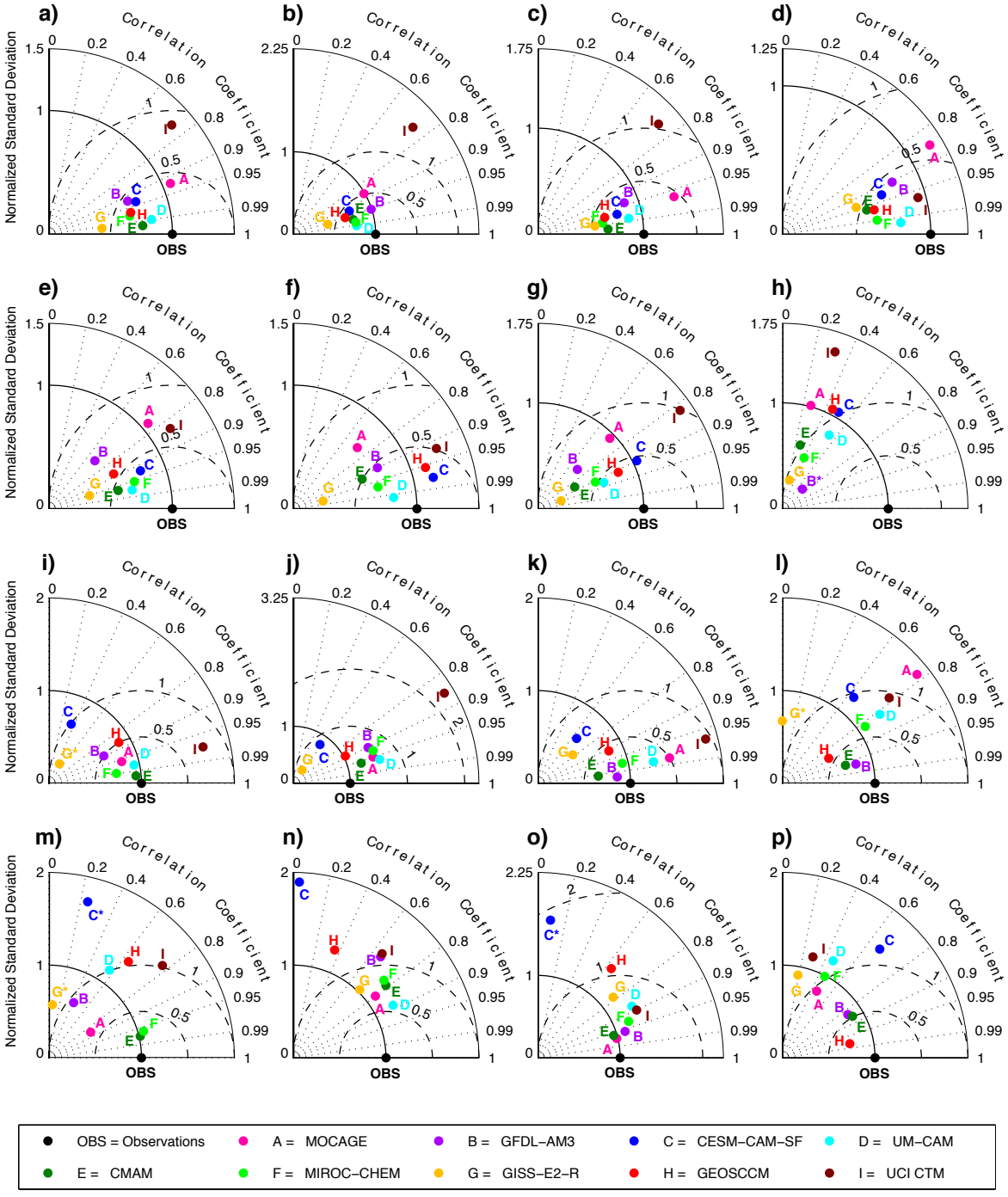

Figure S3. Taylor diagrams comparing the gridded observations of surface O_3 (OBS) to the ACCMIP models (A-H) and the UCI CTM (I) for the (**a-d**) summer (JJA) diurnal cycle, (**e-h**) winter (DJF) diurnal cycle, (**i-l**) annual cycle of MDA8, and (**m-p**) annual cycle of AQX events averaged over (column 1) WNA, (column 2) ENA, (column 3) SEU, and (column 4) NEU. In cases where a model has a negative correlation, it is plotted as being positive and its letter abbreviation is appended with an asterisk.

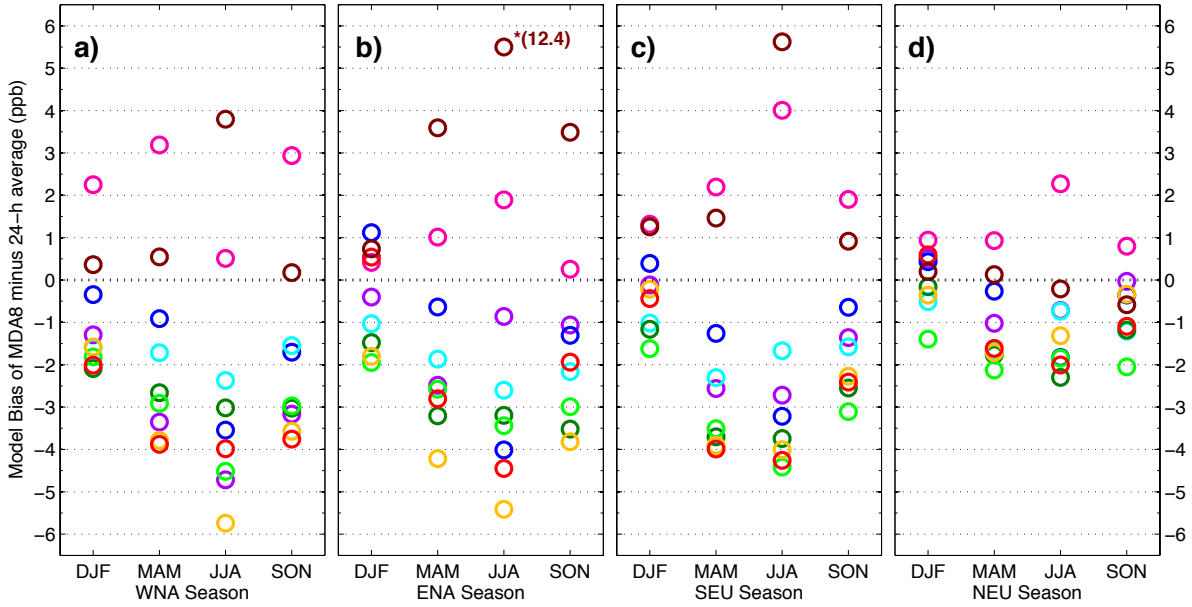

Figure S4. Model biases of MDA8 minus 24 h average O_3 (ppb) in (**a**) WNA, (**b**) ENA, (**c**) SEU, and (**d**) NEU averaged over winter (DJF), spring (MAM), summer (JJA), and fall (SON). The model corresponding to each colored circle can be found in the legend of Figs. 1 and S3. The circle for model I (dark red) in ENA JJA has been arbitrarily placed since its actual value (12.4 ppb) is outside the range shown in the panel.

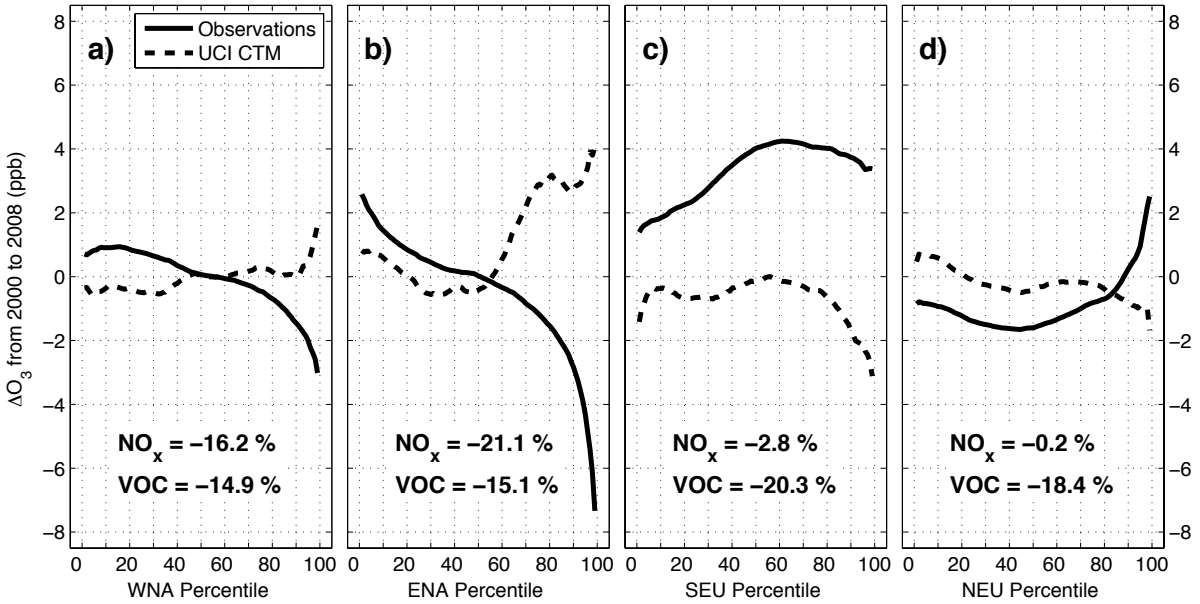

Figure S5. Change in MDA8 O_3 (2008 minus 2000) calculated from a linear fit to the region-wide average MDA8 O_3 corresponding to the 1st to 99th percentiles over (**a**) WNA, (**b**) ENA, (**c**) SEU, and (**d**) NEU for the observations (solid lines) and UCI CTM (dashed lines). The change (%) in NO_x and total non-methane VOC emissions over the period are also given for each region.

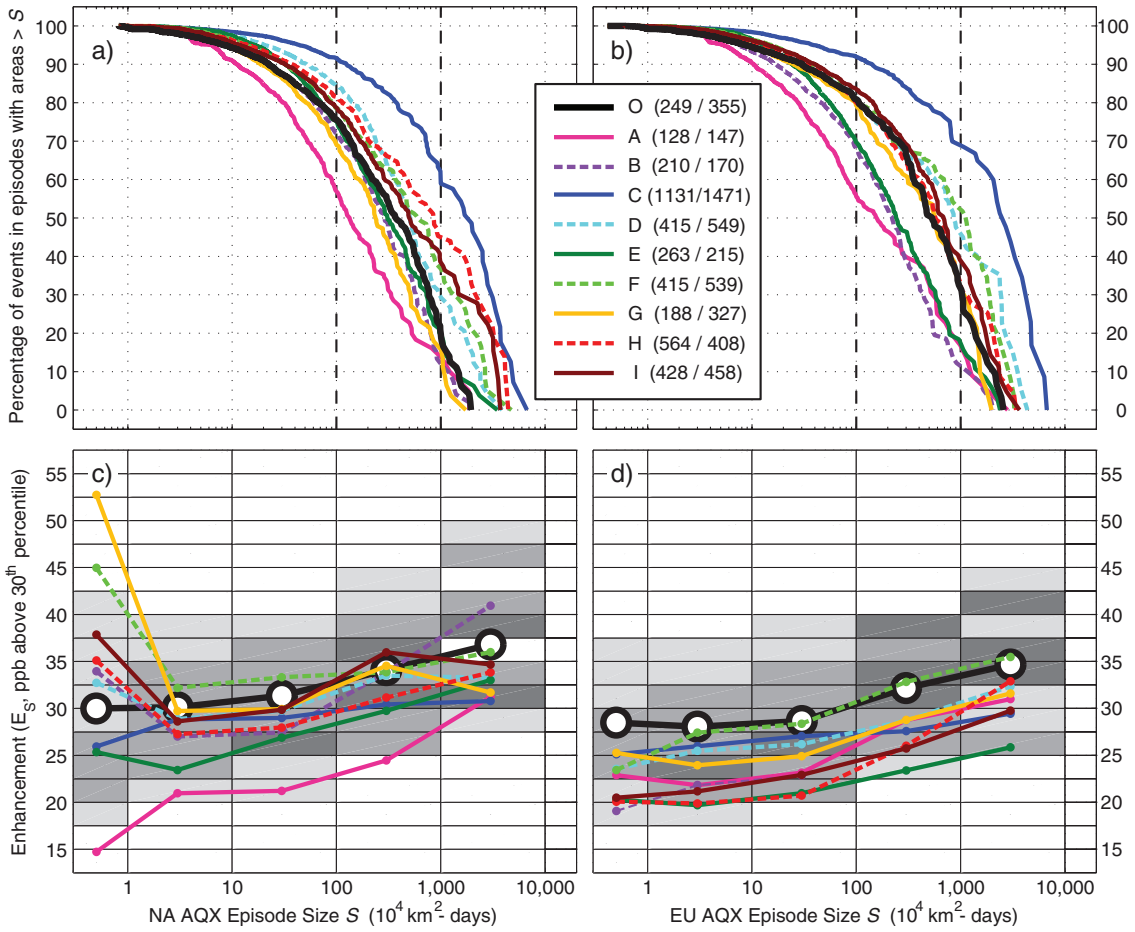

Figure S6. Similar to Fig. 4 but for the 10 AQX events per year case. (**a-b**) Complementary cumulative distribution (CCD) of the percentage of total areal extent of all individual AQX events (10-per-year case) as a function of AQX episode size, (S, 10^4 km^2-days) for the observations (O), ACCMIP models (A-H), and UCI CTM (I) in (**a**) NA and (**b**) EU. Dashed vertical lines show the graphical representations of CCD_{100} and CCD_{1000}. Mean episode size $\overline{S}$ for each dataset and domain is given in the legend as (NA/EU). (**c-d**) Density scatterplot of the observations enhancement of AQX episodes E_S versus their size S (E_S binned at 5 ppb increments from <15 ppb to >55 ppb, S binned at each log-decade) in (**c**) NA and (**d**) EU. The gray scale represents the relative percentage of AQX episodes in each (x, y) = (S, E_S) bin and includes percent ranges of ≤5% (white), 5-10%, 10-15%, and >15% (darkest gray) where the size bins (i.e., columns) are normalized to sum to 100%. The overlain curves show the observation's and each model's area-weighted mean enhancement E_S in each size bin. The values of E_S in each size bin for models A and I have been scaled by 0.5 since they are largely outside the range of the others.

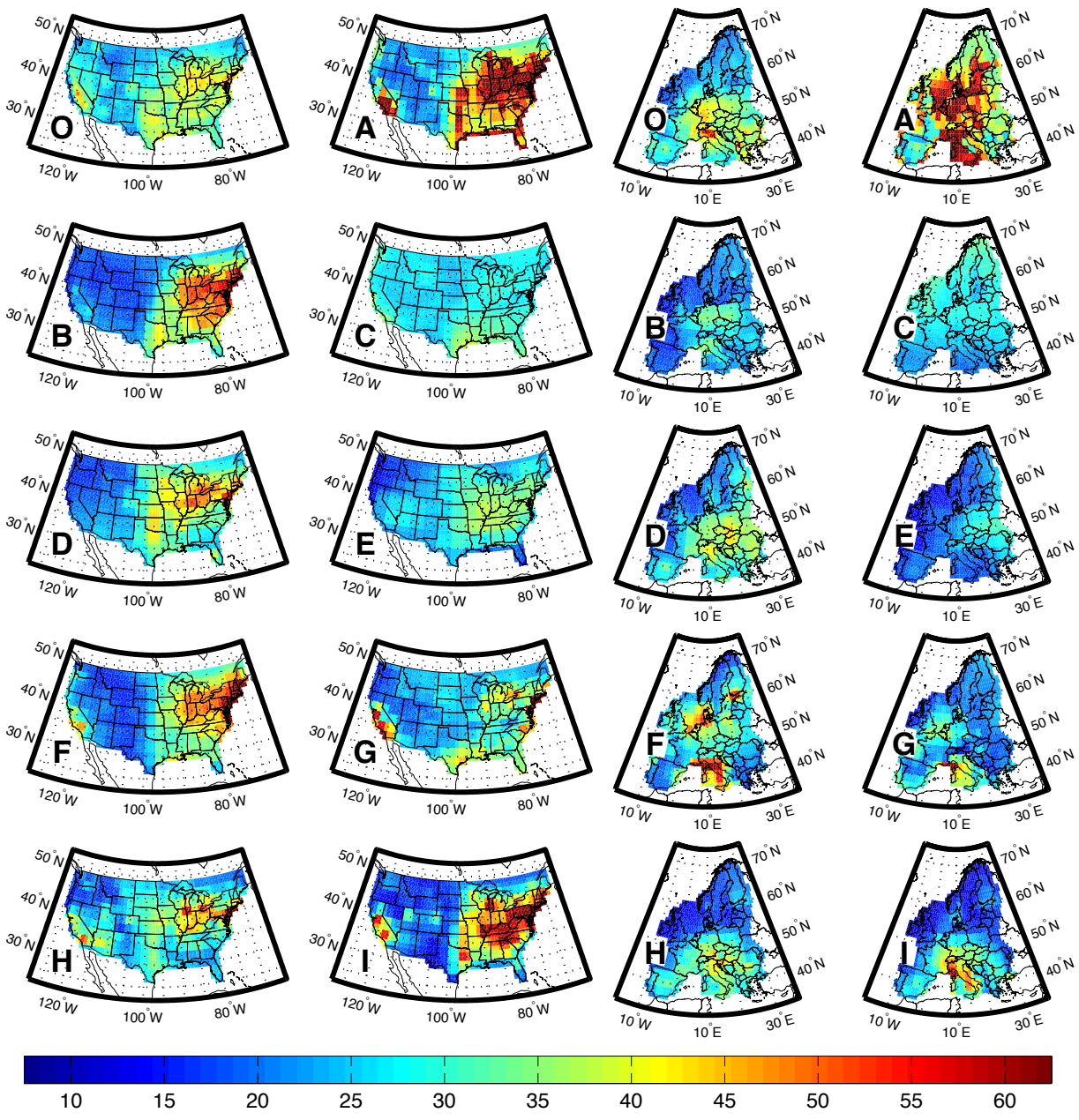

Figure S7. Enhancement at the AQX threshold E_{AQX} = difference between the ~97.3 and 30th percentile of the gridded surface MDA8 O_3 (ppb) over (left two columns) NA and (right two columns) EU for the observations (O), ACCMIP models (A-H), and UCI CTM (I). The values of model I are scaled by 0.5 so the same color scale can be used.